Carbohydrate Polymers 87 (2012) 2120–2128

Contents lists available at SciVerse ScienceDirect

Carbohydrate Polymers

journal homepage: www.elsevier.com/locate/carbpol

Targeted delivery of paclitaxel using folate-conjugated heparin-poly(β-benzyl-L-aspartate) self-assembled nanoparticles

Li Li[a], Jun Ki Kim[b], Kang Moo Huh[a,*], Yong-kyu Lee[b], So Yeon Kim[c,*]

[a] Department of Polymer Science and Engineering, Chungnam National University, Daejeon 305-764, South Korea
[b] Department of Chemical and Biological Engineering, College of Advanced Science and Technology, Chungju National University, Chungju 380-702, South Korea
[c] Department of Chemical Engineering Education, College of Education, Chungnam National University, Daejeon 305-764, South Korea

ARTICLE INFO

Article history:
Received 16 August 2011
Received in revised form 6 October 2011
Accepted 15 October 2011
Available online 20 October 2011

Keywords:
Nanoparticle
Drug delivery
Active targeting
Paclitaxel
Heparin

ABSTRACT

A self-assembled nanoparticulate system composed of a folate-conjugated heparin-poly(β-benzyl-L-aspartate) (HP) amphiphilic copolymer was proposed for targeted delivery of the antineoplastic drug paclitaxel (PTX). PTX was incorporated into three types of heparin-based nanoparticles, including HP, folate-conjugated HP (FHP), and folate-polyethylene glycol (PEG)-conjugated HP (FPHP), using a simple dialysis method. The PTX-loaded nanoparticles were then characterized according to particle size (140–190 nm) and size distribution, drug-loading content and efficiency, and *in vitro* release behavior. In the cellular uptake study using KB cells positive for the folate-receptor (FR), FHP and FPHP nanoparticles showed a much higher cellular uptake than did unconjugated HP nanoparticles. Specifically, when the PEG spacer was inserted between the folate ligand and heparin backbone, FPHP nanoparticles had a greater cellular uptake than did FHP nanoparticles. The *in vitro* cytotoxicity of PTX-loaded HP, FHP, and FPHP nanoparticles was studied in KB cells and FR-negative A549 cells. Compared with the cytotoxicity in A549 cells, PTX-loaded FHP and FPHP nanoparticles exhibited more potent cytotoxicity in KB cells than did PTX-loaded HP nanoparticles and free-PTX, suggesting that the presence of folate enhanced intracellular uptake via FR-mediated endocytosis. In addition, FPHP nanoparticles exhibited much greater cytotoxicity in KB cells than did FHP nanoparticles. These results suggest that PTX-loaded folate-conjugated HP nanoparticles are a potentially useful delivery system for cancer cells positive for the folate-receptor.

1. Introduction

Paclitaxel (PTX) is a diterpenoid isolated from *Taxus brevifolia* and has been approved by the U.S. Food and Drug Administration (FDA) for the treatment of ovarian and breast cancers (Goldspiel, 1997; Panchagnula, 1998). Because of its high hydrophobicity, it is clinically administered dissolved in Cremophor EL and ethanol, which is the only clinical form of PTX available. However, a number of side effects are associated with Cremophor EL, such as hypersensitivity reactions, nephrotoxicity, neurotoxicity, and cardiotoxicity (Liebmann, Cook, Mitchell, & Cremophor, 1993). In order to overcome these limitations, various self-assembled nanoparticulate systems composed of biocompatible and biodegradable amphiphilic copolymers that can physically entrap PTX within the hydrophobic inner core for PTX delivery have been investigated (Huh et al., 2008; Kim, Shin, Lee, Cho, & Sung, 1998; Pan & Feng, 2008). Formulation of PTX using a self-assembled nanoparticle carrier presents several advantages: (i) improves aqueous solubility without the use of a toxic adjuvant; (ii) sustained release prolongs the half-life of the drug; and (iii) enables the drug to passively target tumor tissue via an enhanced permeability and retention (EPR) effect, thus minimizing toxicity to healthy tissue (Kukowska-Latallo et al., 2005; Maeda, Sawa, & Konno, 2001). In addition, the modification of particle surface with active targeting molecules can further enhance the therapeutic efficacy and reduce the side effects of PTX, resulting in a specific effect and high uptake of the drug in tumor cells (de Wolf & Brett, 2000).

Folic acid (folate) is an attractive candidate molecule for use as a targeting ligand. Folate-receptor (FR) is overexpressed in a wide variety of human tumors, including greater than 90% of ovarian carcinomas (Toffoli et al., 1997). Since the affinity between folate and FR is high ($K_d \sim 10^{-10}$ M), conjugates of folic acid have the ability to enter cancer cells expressing the folate receptor via FR-mediated endocytosis. Recently, nano-sized drug carriers containing folate, such as micelles (Du et al., 2010), dendrimers (Chandrasekar, Sistla, Ahmad, Khar, & Diwan, 2007), liposomes (Zhao et al., 2010), and inorganic nanoparticles (Lin et al., 2009) have been widely studied for the selective delivery of therapeutic agents.

* Corresponding authors. Tel.: +82 42 821 5892.
E-mail addresses: khuh@cnu.ac.kr (K.M. Huh), kimsy@cnu.ac.kr (S.Y. Kim).

0144-8617/$ – see front matter © 2011 Elsevier Ltd. All rights reserved.
doi:10.1016/j.carbpol.2011.10.030

In a previous study, we synthesized a self-assembled nanoparticulate system made from a folate-conjugated heparin-poly(β-benzyl-L-aspartate) (HP) amphiphilic copolymer (Li, Huh, Lee, & Kim, 2009). The use of a heparin-based system is of special interest because of its attractive anticancer properties. Recent studies investigating, the inhibitory effects of heparin on tumor growth and metastasis in experimental models showed that heparin interferes with the activity of growth factors such as bFGF and VEGF, resulting in the inhibition of angiogenesis and tumor development (Bobek & Kovarík, 2004; Mousa & Petersen, 2009; Niers et al., 2007; Smorenburg & van Noorden, 2001).

The present study is a continuation of our work to synthesize folate-conjugated HP for targeted delivery of PTX. The anticoagulant activity and *in vitro* cellular uptake of heparin-based nanoparticles were evaluated. In addition, PTX-loading capacity and *in vitro* PTX release kinetics were also investigated. The therapeutic effect of PTX formulated into folate-conjugated HP (with targeting effect) was evaluated *in vitro* by measuring the viability of human nasopharyngeal epidermoid cancer (KB) cells (FR positive cells) and human lung adenocarcinoma epithelial (A549) cells (FR negative cells).

2. Materials and methods

2.1. Materials

Low molecular weight heparin (LMWH, 101 IU/mg, 6000 Da) was obtained from Mediplex Co. (Korea). Paclitaxel (PTX) was provided by Samyang Genex Co. (Daejeon, Korea). Folic acid (folate), polyoxyethylene bis (amine) (PEG-bis (amine)), β-benzyl-L-aspartate (BLA), triphosgene, butylamine, fluorescein-5-isothiocyanate (FITC), and 1-ethyl-3-(3-dimethylaminopropyl) carbodiimide hydrochloride (EDC) were purchased from Sigma–Aldrich Chemical Co. (St. Louis, USA). Coatest anti-Factor Xa assay kits were purchased from Chromogenix (Milano, Italy). Penicillin–streptomycin, fetal bovine serum, 0.25% (w/v) trypsine-0.03% (w/v) ethylenediaminetetraacetic acid (EDTA) solution and EMGM medium were purchased from American Type Culture Collection (Rockville, MD). RPMI-1640 medium (without folate) was obtained from Invitrogen (Carlsbad, CA). Spectra/Por membranes were purchased from Spectrum Laboratories, Inc. (Rancho Dominguez, USA). All chemicals were analytical grade and were used without further purification.

2.2. Synthesis and characterization of heparin-based amphiphilic copolymers

Poly(β-benzyl-L-aspartate) (PBLA), amine-terminated folate (folate-NH_2) and folic acid-conjugated poly(ethylene glycol) (folate-PEG) were synthesized as described in our previous report (Li et al., 2009). Here, three types of heparin-based copolymers with or without folate ligands were synthesized, including heparin-PBLA (HP), folate-heparin-PBLA (FHP) and folate-PEG-heparin-PBLA (FPHP) copolymers. Briefly, heparin (200 mg) dissolved in 5 mL of formamide was reacted with folate-NH_2 (or folate-PEG) and EDC (95.8 mg) at room temperature for 24 h to obtain folate-conjugated heparin (FH) and folate-PEG-conjugated heparin (FPH). Then a dialysis (molecular weight cut-off (MWCO) 2000 for FH, MWCO 5000 for FPH) was performed against 0.1 M sodium bicarbonate and deionized water for 2 days, respectively. Heparin, FH and FPH were sequentially reacted with PBLA as follows: heparin, FH, and FPH were dissolved in 5 mL of formamide, and each solution was then mixed with EDC (95.8 mg) and PBLA dissolved in 5 mL of dimethylformamide (DMF). The feed ratios of folate-NH_2 (or folate-PEG)/heparin/PBLA are listed in Table 1. The coupling reaction was allowed to proceed at room temperature for 36 h under nitrogen. The obtained solution was dialyzed for two days, lyophilized, washed with acetone to remove the unreacted PBLA and dried under vacuum.

The chemical compositions of the HP, FHP and FPHP copolymers were determined using the colorimetric method (Li et al., 2009). The anticoagulant activity of these copolymers was evaluated using a chromogenic anti-Factor Xa assay. The critical micelle concentration (CMC) of the copolymers was determined using fluorescence spectroscopy with a pyrene probe as described in our previous study (Li et al., 2009).

2.3. Preparation and characterization of PTX-loaded HP, FHP and FPHP nanoparticles

PTX-loaded HP, FHP and FPHP nanoparticles were prepared using the dialysis method. Briefly, 100 mg of copolymer and 10 mg of PTX were dissolved in 5 mL of dimethyl sulfoxide (DMSO). The solution was stirred for 2 h in the dark to obtain an optical transparent solution and then dialyzed against deionized water for 48 h using a Sectra/Por dialysis membrane (MWCO, 2000). To remove unloaded aggregated PTX, the resultant solution was filtered through a 0.45 μm filter and then lyophilized.

The loading content of PTX was determined using HPLC (Agilent 1100 series, Agilent Technologies, USA). The mobile phase consisted of acetonitrile/water (55:45, v/v) with a flow rate of 1.0 ml/min. The PTX-loading amount was determined using a calibration curve of various PTX concentrations (0.1–100 μg/mL) versus integrated area (mAU S) at 227 nm. The drug loading content (LC) and drug loading efficiency (LE) were calculated using the following equations:

$$\mathrm{LC} = \frac{\text{mass of PTX in nanoparticle}}{\text{mass of PTX-loaded nanoparticle}} \times 100$$

$$\mathrm{LE} = \frac{\text{mass of PTX in nanoparticle}}{\text{mass of feeding PTX}} \times 100$$

Table 1
Characterization of HP, FHP and FPHP amphiphilic copolymers.

Sample	Polymer type	Feed molar ratio[a]	Coupling ratio[b]	Absolute anti-coagulant activity[c] (IU/mg)	Size[d] (nm)	Polydispersity index	Zeta-potential (mV)	CMC (mg/L)
HP1	Heparin:PBLA	1:3	1:2.66	85.6	51.3 ± 2.0	0.12 ± 0.02	−44.1 ± 1.3	6.67
HP2	Heparin:PBLA	1:6	1:4.35	70.5	66.6 ± 1.3	0.13 ± 0.02	−41.6 ± 2.2	1.65
FHP1	FA:heparin:PBLA	3:1:3	2.12:1:1.98	57.1	63.7 ± 3.8	0.17 ± 0.03	−32.8 ± 1.3	10.94
FHP2	FA:heparin:PBLA	3:1:6	2.12:1:3.60	50.9	66.4 ± 3.7	0.16 ± 0.02	−29.5 ± 1.5	4.57
FPHP1	FA-PEG:heparin:PBLA	3:1:3	2.91:1:1.89	50.1	105.8 ± 1.7	0.11 ± 0.01	−23.9 ± 1.9	41.68
FPHP2	FA-PEG:heparin:PBLA	3:1:6	2.91:1:3.87	45.8	133.7 ± 0.3	0.10 ± 0.02	−21.8 ± 0.6	19.53

[a] The average molecular weights of heparin, PBLA and PEG were 6000, 4890 and 3350 Da, respectively.
[b] The coupling ratio was determined using a colorimetric method.
[c] Evaluated using the Factor Xa chromogenic assay. The absolute anti-coagulant activity of native heparin is 101 IU/mg.
[d] *z*-Average diameter; determined through a dynamic light scattering study.

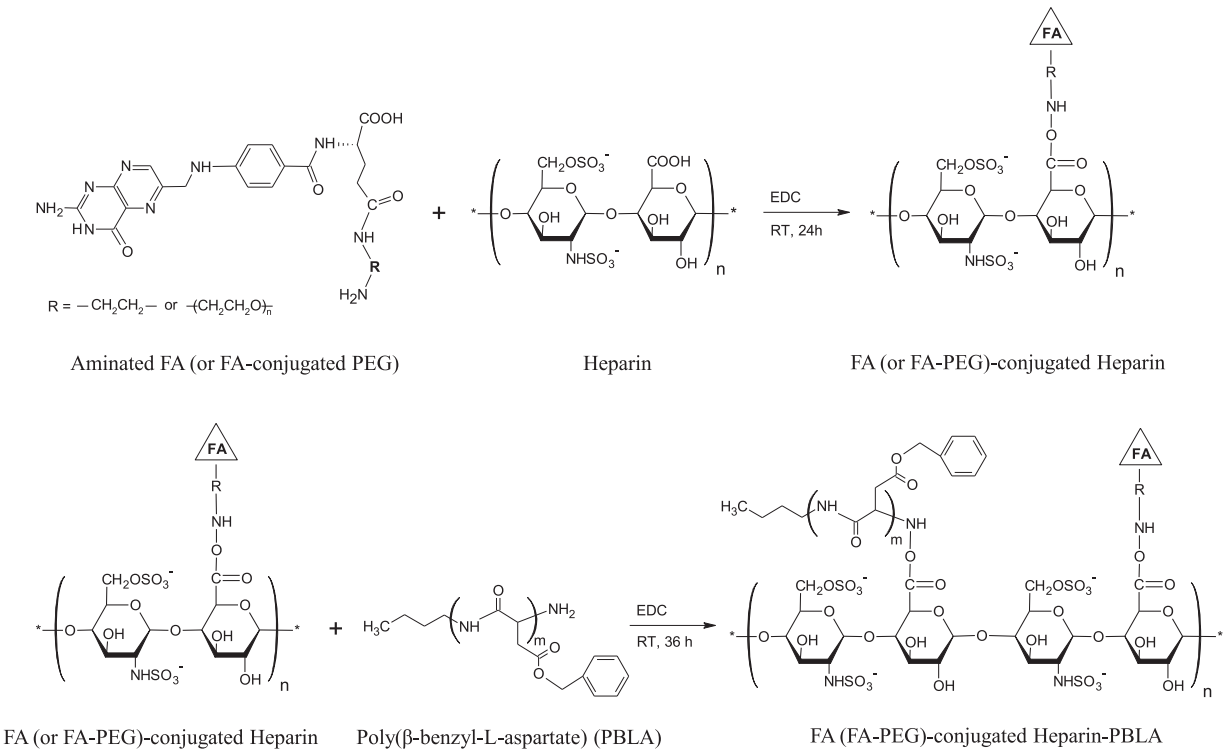

Fig. 1. Synthesis and schematic structure of folate-conjugated HP copolymer.

The size and size distribution of PTX-free and PTX-loaded HP, FHP and FPHP nanoparticles in aqueous solution were determined using dynamic light scattering (DLS) (ELS-Z, OTSUKA, Japan) at an angle of 165° and a temperature of 25 °C using a semi-conductor laser (655 nm) as a light source. All samples were prepared in deionized water at a concentration of 0.2 mg/mL and were filtered through a 0.45 μm syringe filter prior to measurement. The morphologies of PTX-free and PTX-loaded nanoparticles were observed using a field emission scanning electron microscope (FE-SEM) (JSM-7000F, JEOL, Japan) at 15 kV.

2.4. In vitro drug release study

Lyophilized PTX-loaded nanoparticles (2 mg) were suspended in 2 mL of phosphate buffered saline (PBS, 0.01 M, pH 7.4), and sonication was carried out to produce an optically clear solution. The solutions containing PTX-loaded nanoparticles were placed into dialysis bags (MWCO, 2000) containing 35 mL of PBS and were incubated in a 37 °C water bath with gentle shaking at 50 rpm. At predetermined intervals, buffered solutions were collected and replaced with an equivalent volume of fresh PBS. The amount of PTX released was determined using HPLC as described in Section 2.3.

2.5. Cellular uptake study with HP, FHP, and FPHP nanoparticles

To investigate the cellular uptakes of HP, FHP and FPHP nanoparticles, FITC (5 mg) was conjugated to HP2, FHP2, or FPHP2 copolymers (50 mg) in 10 mL of DMSO for 12 h at room temperature. Unbound FITC was removed via dialysis against 0.5 M sodium bicarbonate solution over three days. The cellular uptakes of FITC-labeled HP, FHP, and FPHP nanoparticles were evaluated in KB cells (FR positive) using confocal laser scanning microscopy (CLSM). In brief, each sample of FITC-labeled HP, FHP, and FPHP nanoparticles was dispersed in RPMI-1640 medium at 0.05 mg/mL, added to the cells and incubated for 1 h. The cells were then washed three times with PBS and fixed with 4% formaldehyde in PBS. Cell images were collected using CLSM (Zeiss LSM510, Germany) at excitation and emission wavelengths of 488 and 510 nm, respectively.

2.6. Cytotoxicity study

KB and A549 cells were obtained from the Korean Cell Line Bank. The cells were cultured at 37 °C in RPMI-1640 containing 10% fetal calf serum under a humidified atmosphere containing 5% CO_2. The cells were seeded in 96-well plates at a density of 1×10^4 viable cells per well and were preincubated for 24 h to allow cell attachment. The cells were then incubated with free-PTX and PTX-loaded HP, FHP and FPHP nanoparticles (PTX concentrations of 0.01, 0.1, 1, 10 μg/mL) for 24, 48 or 72 h. At each time point, 100 μL of medium containing 20 μL of methylthiazol tetrazolium (MTT) solution was added to each well, and the plate was incubated for an additional 4 h, followed by the addition of 100 μL of MTT solubilization solution (10% Triton X-100 plus 0.1 N HCl in anhydrous isopropanol; Sigma, Milwaukee, WI) to each well. The solution was gently mixed to dissolve the MTT formazan crystals, and the absorbance of each well was measured with a microplate reader at a wavelength of 570 nm. The background absorbance of the wells was measured at 690 nm and subtracted from the 570 nm measurement. Untreated cells were used as the control and represented 100% viability. Cell viability was expressed as a percentage of a control that had not been treated with nanoparticles, using the following equation:

$$\text{Viability}\,(\%) = \frac{N_i}{N_c} \times 100$$

where N_i and N_c are the number of surviving cells in the group treated with paclitaxel-loaded nanoparticles and in the untreated cell group, respectively.

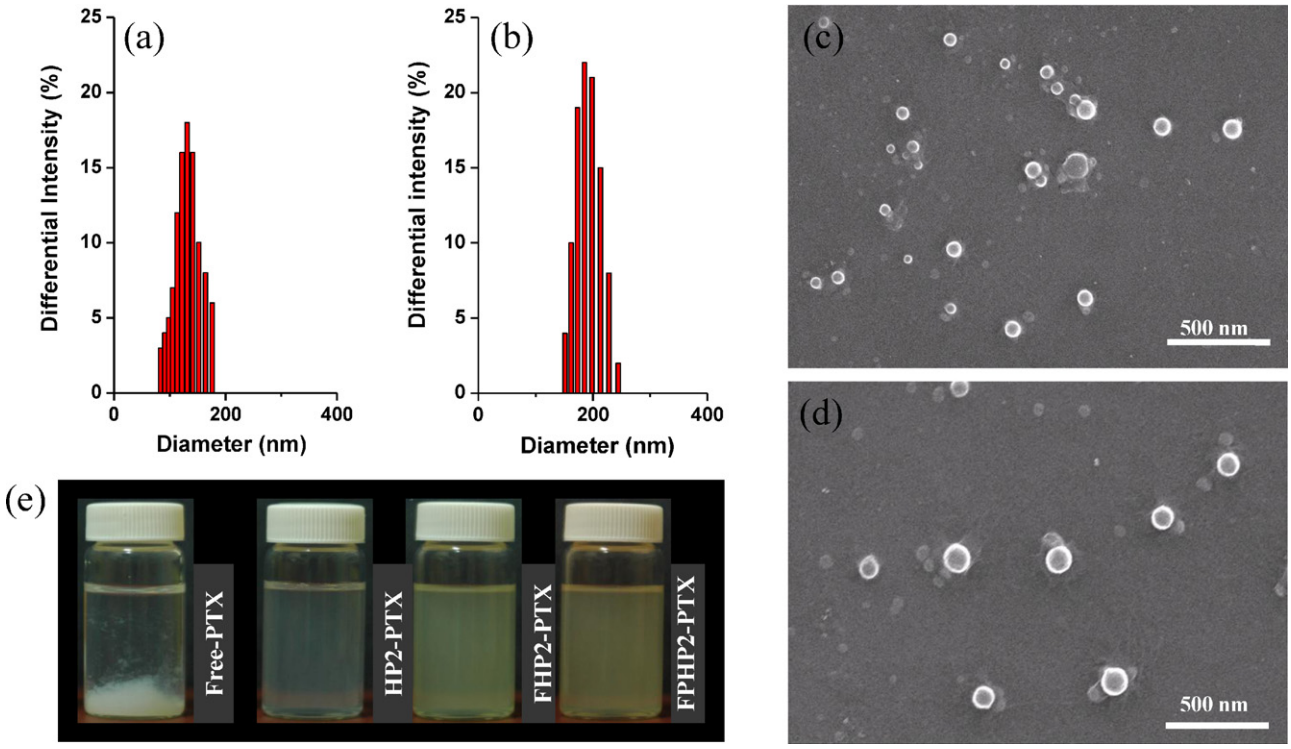

Fig. 2. Typical size distribution of FPHP2 nanoparticles without or with PTX loading, (a) FPHP2 and (b) FPHP2-PTX; field emission scanning electron microscopic (FE-SEM) images of FPHP nanoparticles without or with PTX loading, (c) FPHP2 and (d) FPHP2-PTX; (e) photographic images of PTX suspended in DI water and solubilized with HP, FHP, and FPHP nanoparticles, the concentration of PTX in each vial was 1.5 mg/mL, the solutions were incubated at 37 °C for 24 h.

2.7. Statistical analysis

Statistical differences were performed using one-way ANOVA. Data were presented as mean ± standard deviation. p-Values <0.05 were considered as statistically significant.

3. Results and discussion

3.1. Characterization of HP, FHP and FPHP copolymers

Heparin is well-known for its anticoagulant property due to its ability to accelerate the rate at which antithrombin inhibits serine proteases in the blood coagulant cascade (Linhardt, 1991). In addition to its anticoagulant activity, the multiple antitumor properties, including inhibition of tumor angiogenesis, interference with tumor cell adhesion, and suppression of tumor cell invasion, have been deeply investigated in experimental models in last decade (Niers et al., 2007). Since low molecular weight heparin is more effective than unfractionated heparin in inhibiting VEGF- and bFGF-mediated angiogenesis (Mousa & Petersen, 2009), the heparin used in this study was low molecular weight heparin with average molecular weight of 6000 Da.

The synthetic procedures used to produce HP, FHP, and FPHP copolymers are shown in Fig. 1. The characterizations of these molecules were described in detail in our previous study (Li et al., 2009). Briefly, folate (or folate-PEG) and PBLA were conjugated to a heparin backbone through covalent amide bonds, as confirmed by proton nuclear magnetic resonance (^{1}H NMR) spectroscopy. As shown in Table 1, three types of heparin-based copolymers, HP, FHP and FPHP, were synthesized by varying the feed molar ratios of PBLA and heparin (or FH or FPH). In order to conjugate FA ligands to the HP copolymers, we inserted PEG as a linker between the FA ligands and heparin to extend the length of the ligands. This design is expected to enhance cellular uptake compared to that of direct coupling of folate to heparin. The coupling ratios of folate and folate-PEG to the FHP and FPHP copolymers were 2.12 and 2.91, respectively. The HP, FHP and FPHP copolymers formed self-assembled nanoparticles in aqueous media with mean diameters of about 50–130 nm and a strong negative surface charge (−20 to −45 mV). Fig. 2a and c shows the size distribution and shape of the FPHP2 nanoparticles, as measured using DLS and FE-SEM, respectively.

The SEM measurements shown in Fig. 2c confirmed the synthesis of spherical FPHP2 nanoparticles. The CMC of each copolymer was determined using pyrene as a fluorescence probe. As shown in Table 1, HP, FHP and FPHP copolymers can form stable self-assembled nanoparticles at low concentration. Because intravenous injection of nanoparticle solutions is associated with extreme dilutions by circulating blood, the low CMC values suggest that the HP, FHP and FPHP nanoparticles are stable for systemic PTX delivery. As shown in Table 1, the modification of carboxylic acid groups in heparin results in low anticoagulant activity compared with that of native heparin; the anticoagulant activities of the HP, FHP and FPHP copolymers ranged from 45.8 to 85.6 IU/mg, which are significantly lower than that of unmodified heparin (101 IU/mg). The reduction in anticoagulant activity with heparin-based copolymers is advantageous because heparin-induced side effects following the administration of heparin, such as hemorrhage, thrombocytopenia and osteoporosis hemorrhage, may be effectively inhibited.

3.2. Characterizations of PTX-loaded HP, FHP and FPHP nanoparticles

The poorly water-soluble anticancer drug PTX was physically incorporated into HP, FHP and FPHP nanoparticles using a simple dialysis method. Actually, there are several methods can be used to incorporate hydrophobic drugs into self-assembled nanoparticle

Table 2
Characterization of PTX-loaded nanoparticles.

Sample[a]	Size (nm)	Polydispersity index	LC (%)[b]	LE (%)[c]
HP1-PTX	140.0 ± 1.3	0.11 ± 0.01	4.62 ± 0.02	48.4
HP2-PTX	148.2 ± 6.8	0.13 ± 0.02	5.66 ± 0.06	60.0
FHP1-PTX	149.2 ± 3.6	0.18 ± 0.03	2.69 ± 0.04	27.6
FHP2-PTX	178.3 ± 3.5	0.16 ± 0.03	5.28 ± 0.05	55.7
FPHP1-PTX	190.5 ± 4.7	0.12 ± 0.02	4.88 ± 0.06	51.3
FPHP2-PTX	193.8 ± 3.3	0.12 ± 0.01	5.34 ± 0.05	56.4

[a] The feed ratio of PTX/copolymer was fixed at 1/10.
[b] LC = (mass of PTX in nanoparticle/mass of PTX-loaded nanoparticle) × 100.
[c] LE = (mass of PTX in nanoparticle/mass of feeding PTX) × 100.

cores, the final degree of drug loading may depend on the loading technique. However, due to the limited solubility of HP, FHP and FPHP copolymers in volatile organic solvents, the dialysis method was the best choice for incorporation of PTX in self-assembled HP, FHP and FPHP nanoparticle cores. During the dialysis process, a gradual replacement of the organic solvent with water triggers self-assembly of hydrophobic PBLA blocks accompanied by entrapment of PTX in the self-aggregate cores. As shown in Fig. 2e, opalescent and homogenous solutions were obtained after the dialysis process, indicating effective solubilization of PTX. PTX was entrapped in self-assembled nanoparticles through the hydrophobic interaction between PTX and the PBLA core of the nanoparticle.

Table 2 shows the characterizations of HP, FHP and FPHP nanoparticles containing physically entrapped PTX. These

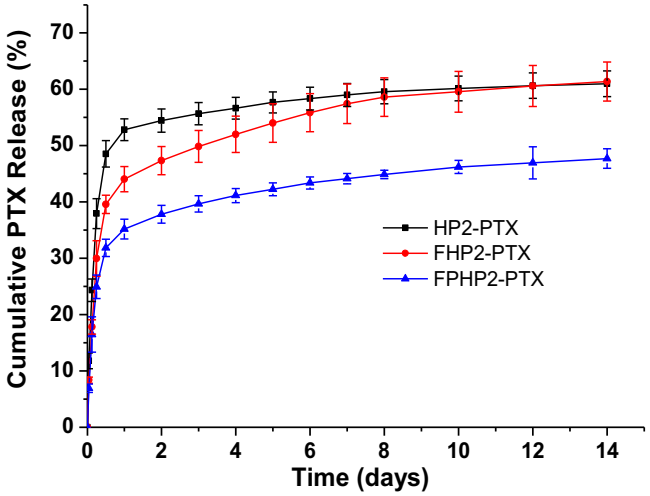

Fig. 3. Cumulative PTX release profiles from PTX-loaded HP, FHP and FPHP nanoparticles in PBS (pH 7.4) (mean ± S.D., $n = 3$).

nanoparticles efficiently solubilized PTX at a LC level of 2.69% to 5.66% (wt/wt), depending on the composition of the copolymer and the coupling ratio of PBLA. The PTX loading capacity of HP, FHP and FPHP nanoparticles were found relatively lower than that of some micellar systems (Du et al., 2010; Huh et al., 2008; Kim et al.,

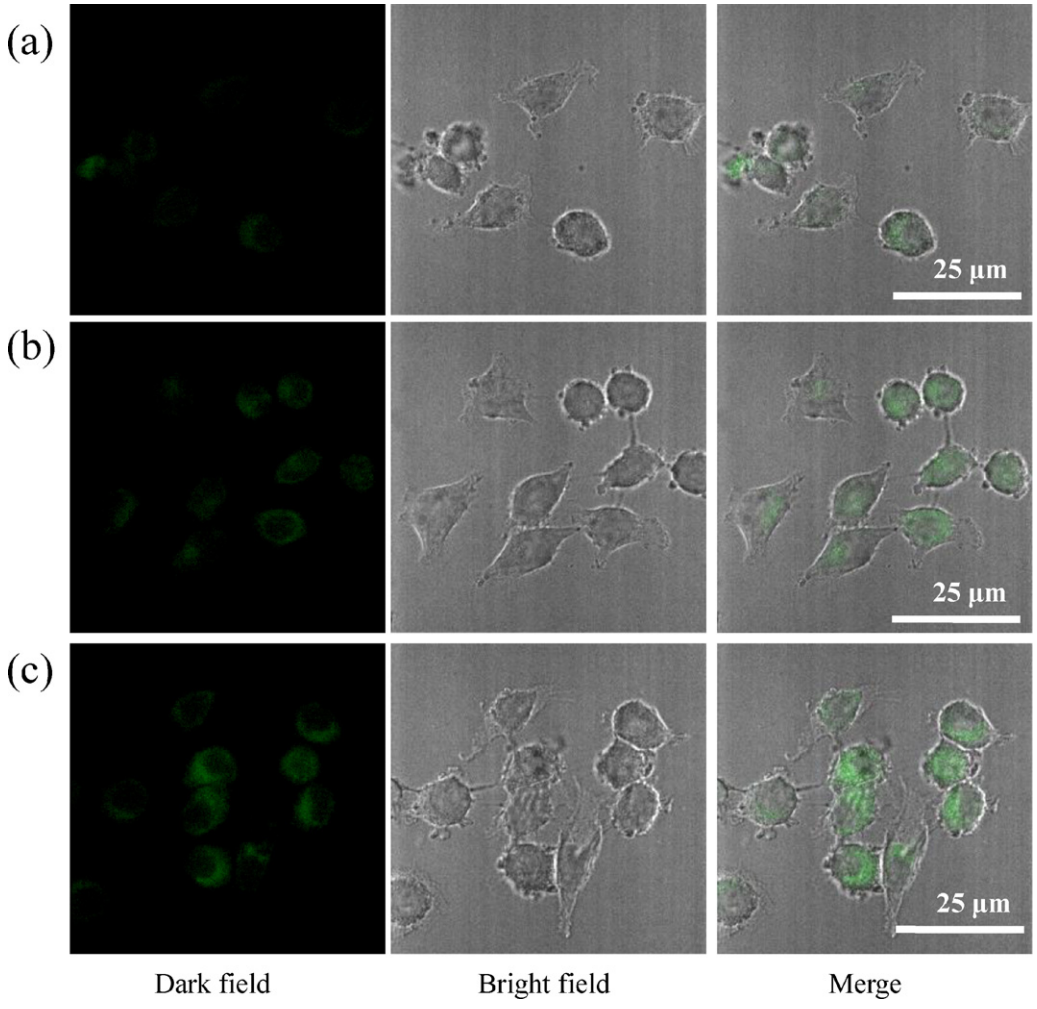

Fig. 4. CLSM images of KB cells incubated with (a) FITC-HP, (b) FITC-FHP, and (c) FITC-FPHP.

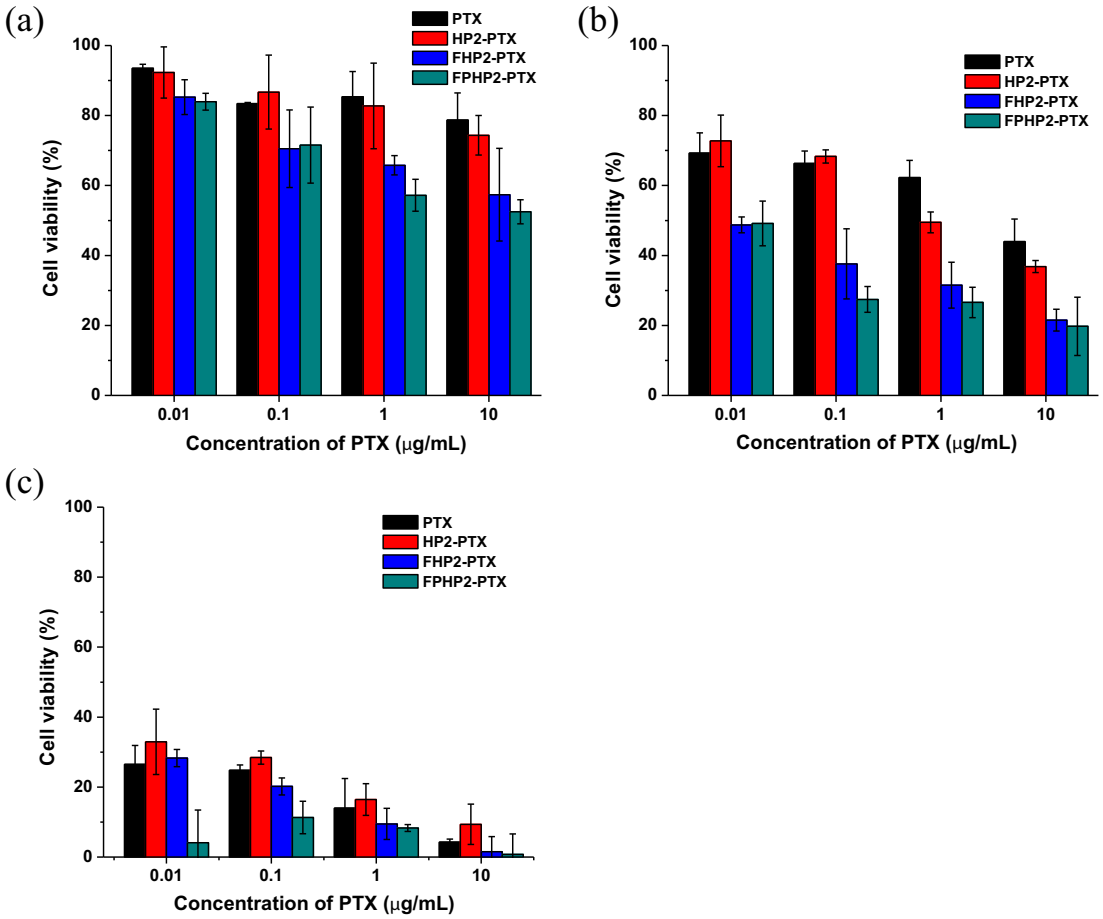

Fig. 5. Cell viabilities of KB cell lines after incubation with PTX, HP2-PTX, FHP2-PTX and FPHP2-PTX nanoparticles for (a) 24 h, (b) 48 h and (c) 72 h (mean ± S.D., $n = 6$).

1998), whereas were relatively higher than that of some micellar systems, such as core-cross-linked PEG-poly(ε-caprolactone) micelle (Shuai, Merdan, Schaper, Xi, & Kissel, 2004) and poly(ethyl ethylene phosphate)-poly(ε-caprolactone) micelle (Wang, Tang, Li, Xiong, & Wang, 2008). For each type of heparin-based nanoparticle, the copolymer with a higher PBLA coupling ratio showed a favorable drug loading capacity, presumably due to the existence of more hydrophobic chains available for drug encapsulation. For example, FHP2-PTX (coupling ratio of heparin/PBLA/FA = 1/3.60/2.12, LC = 5.28%) showed about twofold more LC than FHP1-PTX (coupling ratio of heparin/PBLA/FA = 1/1.98/2.12, LC = 2.69%). The LCs of HP2-PTX, FHP2-PTX and FPHP2-PTX were 5.66%, 5.28%, and 5.34%, respectively. This indicates that the conjugation of FA or FA-PEG to the heparin backbone did not have a significant effect on LC. The effects of drug loading on particle size and size distribution were also studied using DLS. The particle size increased when PTX was incorporated, as shown in Tables 1 and 2. However, the particle size of PTX-loaded nanoparticles ranged from 140 to 190 nm, and the size distribution was narrow (Fig. 2b). Because of their small sizes, these PTX-loaded nanoparticles are considered suitable for passive delivery of PTX to targeted tumors through the EPR effect. The morphologies of PTX-loaded nanoparticles were examined using FE-SEM. As shown in Fig. 2d, FPHP2-PTX nanoparticles have a well-defined spherical shape with increased particle size after drug loading.

3.3. In vitro drug release

Fig. 3 shows the *in vitro* release profiles of PTX from three kinds of drug-loaded nanoparticles, HP2-PTX, FHP2-PTX and FPHP2-PTX. The release profiles featured a rapid release at the initial stage, followed by a smooth, sustained release. This biphasic release profile is the typical pattern for PTX-loaded self-assembled nanoparticles, as observed by other groups (Du et al., 2010; Huh et al., 2008; Kim et al., 1998; Wang et al., 2008). The initial fast release may be ascribed to the dissolution and diffusion of drug that was not compactly loaded in the cores of the nanoparticles, while the slower, sustained release may be from the diffusion of the drug inside the nanoparticles or may be facilitated by water-mediated erosion of the polymer matrix. Within 14 days, about 60%, 61% and 47% of PTX were released from HP2, FHP2 and FPHP2 nanoparticles, respectively. The presence of PEG chains in the FPHP copolymer led to a slower release of PTX from the nanoparticles. The introduction of long PEG chains on a heparin backbone may produce a steric exclusion effect for drug release, thus inhibiting drug escape from the polymer matrix.

3.4. Cellular uptake of HP, FHP and FPHP nanoparticles

Human nasopharyngeal epidermoid cancer (KB) cells were used to evaluate the cellular uptakes of HP, FHP, and FPHP nanoparticles. KB cells express a high level of FR on the surfaces of their cellular membranes because they require folate for growth and proliferation (Leamon, Cooper, & Hardee, 2003; Saul, Annapragada, Natarajan, & bellamkonda, 2003). Therefore, the capacity of FHP2 and FPHP2 nanoparticles for target recognition was evaluated in these cells. For comparison, cells were also treated with non-folate HP2 nanoparticles under identical conditions. As shown in Fig. 4a, the cells treated with FITC-HP2 nanoparticles showed weak

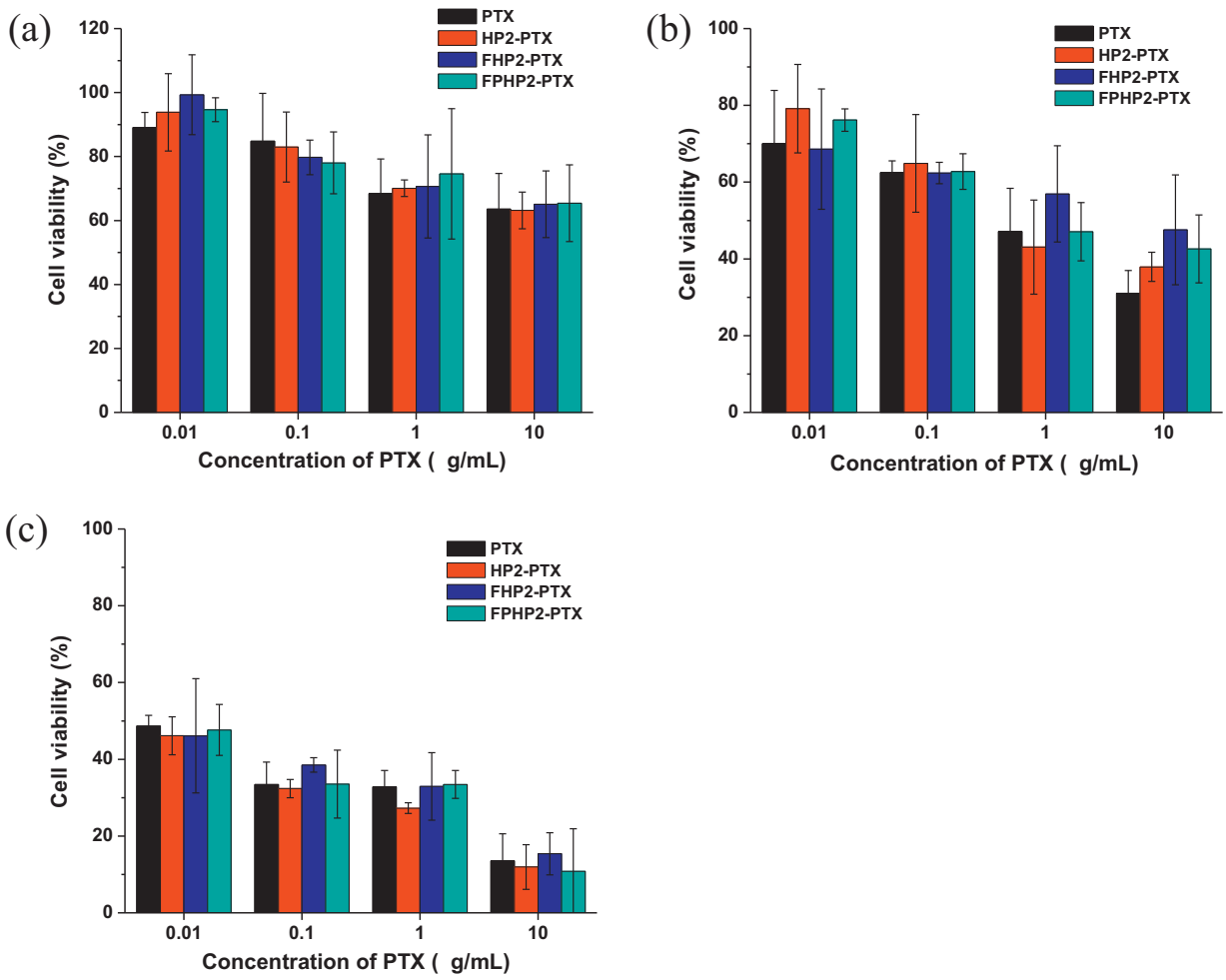

Fig. 6. Cell viabilities of A549 cell lines after incubation with PTX, HP2-PTX, FHP2-PTX and FPHP2-PTX nanoparticles for (a) 24 h, (b) 48 h and (c) 72 h (mean ± S.D., $n = 6$).

fluorescence signals, suggesting a low non-specific intracellular uptake. In contrast, the cells treated with FITC-FHP2 and FITC-FPHP2 nanoparticles showed high intracellular FITC signals.

The uptake putatively results from a specific interaction between the folate-conjugated FHP and FPHP nanoparticles and the FR on KB cells; thus, endocytosis of FHP and FPHP nanoparticles occurs through a rapid receptor-mediated pathway. This indicates that FHP and FPHP nanoparticles could be used to target cancer cells over-expressing FR. We also noted that the FPHP2 nanoparticles showed stronger FITC signals than did FHP2 nanoparticles (Fig. 4b and c); suggesting a higher uptake of FPHP nanoparticles in KB cells compared to that of FHP nanoparticles.

The introduction of PEG chains was expected to increase the length between folate ligands and the heparin backbone since PEG may extend the folate ligands further from the particle surface. This special design could aid in nanoparticle recognition by the FR. On the other hand, the highly negatively charged surfaces of heparin-based nanoparticles may limit the interactions between nanoparticles and the cell membrane; the conjugation of FA-PEG on the heparin backbone decreased the negative surface charge of the nanoparticle compared with that produced with FHP. For example, the zeta-potentials of FHP2 and FPHP2 were −29.5 mV and −21.8 mV, respectively. Thus, FPHP nanoparticles may have a favorable surface charge, allowing for better uptake.

3.5. *In vitro cytotoxicity study*

The *in vitro* cytotoxicities of free-PTX, HP2-PTX, FHP2-PTX and FPHP2-PTX were studied in KB (FR-positive) and A549 (FR-negative) cells. Cell viability was determined using the MTT assay after treatment with the sample suspensions for 24 h, 48 h and 72 h. Generally, both free-PTX and the three types of PTX-loaded nanoparticles showed dose-dependent and time-dependent cytotoxicity, as shown in Figs. 5 and 6. In FR-positive KB cells, HP2-PTX nanoparticles and free-PTX should be transported into cells via endocytosis and passive diffusion, respectively. However, FHP2-PTX and FPHP2-PTX nanoparticles are likely to be internalized via receptor-mediated endocytosis; thus, FHP2-PTX and FPHP2-PTX exhibit superior cytotoxic activities compared to those of PTX and HP2-PTX ($p < 0.05$). For example, the viability of KB cells treated with free-PTX and HP2-PTX was around 70% (incubation time 48 h, 0.1 μg/mL of PTX equiv.), and the cell viabilities of cells treated with FHP2-PTX and FPHP2-PTX were 28.4% and 39.6%, respectively; around twofold lower than those of free-PTX and HP2-PTX.

In contrast, there was no significant difference in cytotoxicity among free-PTX and PTX-loaded nanoparticles in the FR-negative A549 cells at most of the concentrations tested ($p < 0.05$) (Fig. 7). These results suggested that folate moieties in the FHP2-PTX and FPHP2-PTX nanoparticles play an important role in enhancing the cytotoxic effect by binding to the FR on KB cells and subsequently increasing their intracellular uptake as a result of receptor-mediated endocytosis.

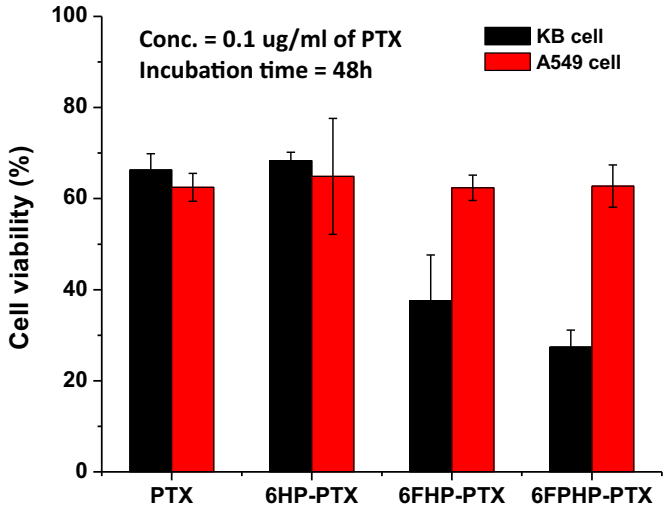

Fig. 7. Enhanced cytotoxic effect of folate-conjugated PTX-loaded nanoparticles compared with cell viability in KB and A549 cells (mean ± S.D., $n = 3$) (conc. of PTX = 0.1 μg/mL, incubation time = 48 h).

It is worth noting that the FPHP2-PTX nanoparticles showed a higher cytotoxic effect in KB cells than did the FHP2-PTX at most of the concentrations tested ($p < 0.05$). For example, when the KB cells were incubated for 48 h (with an equivalent PTX concentration of 0.1 μg/mL) the viabilities of FHP2-PTX- and FPHP2-PTX-treated cells were 28.4% and 39.6%, respectively (Fig. 7). Since the import of PEG spacers significantly enhanced the cellular uptake of FPHP nanoparticles (see Section 3.4), the PTX-loaded FPHP nanoparticles should be more easily and efficiently transported into cells. As a result, the FPHP2-PTX nanoparticles exhibited higher cytotoxicity in KB cells than did the FHP2-PTX.

In summary, enhanced *in vitro* cytotoxicity of PTX-loaded FHP and FPHP nanoparticles suggests that an active tumor targeting approach using a folate-conjugated HP nanoparticle system could increase tumor specificity and decrease the required dosage of PTX *in vivo*. Thus, folate-conjugated HP nanoparticles have the potential to serve as drug carriers for tumor targeted delivery of hydrophobic drugs, such as PTX, for cancer therapy.

4. Conclusions

HP, FHP and FPHP copolymers were synthesized for physical entrapment of the hydrophobic anticancer drug PTX. These copolymers can form nano-sized particles (50–130 nm) in an aqueous medium at low concentration and with negatively charged surfaces. The reduced anticoagulant activity enabled them to serve as a safe anticancer drug carrier in clinical applications. Hydrophobic PTX was efficiently incorporated into self-assembled nanoparticles using a dialysis method. Although particle size increased after drug loading, it was still less than 200 nm; thus, drug-loaded nanoparticles may enable passive targeting to the tumor site through the EPR effect.

The *in vitro* drug release studies showed that both of the PTX-loaded nanoparticles exhibited a typical biphasic release pattern. The cellular uptake study in KB cells revealed that FHP and FPHP nanoparticles could serve as active targeting carriers for cancer cells overexpressing FR. The PTX-loaded HP nanoparticles and PTX showed similar cytotoxicities in KB and A549 cells, whereas PTX-loaded-FHP and -FPHP nanoparticles showed higher and more selective cytotoxicity in KB cells compared with those in A549 cells. It was also found the cellular uptake efficiency of FPHP and the cytotoxicity of FPHP-PTX nanoparticles were much higher in KB cells than were those of the FHP and FHP-PTX nanoparticles. The PEG spacer introduced between the folate ligand and the heparin backbone of the FPHP and FPHP-PTX nanoparticles may increase the length of the targeting moiety, thus enabling the nanoparticles to be more easily and effectively recognized by the FR. These findings suggested the FPHP nanoparticles have great potential to serve as PTX carriers for tumor targeted therapy.

Acknowledgements

This work was supported by the Korea Research Foundation Grant funded by the Korea Government (MOEHRD) (KRF-2007-531-D00003). This work was partially supported by the National Research Foundation of Korea (NRF) grant funded by the Korea Government (MEST) (2010-0029536).

References

Bobek, V. & Kovarík, J. (2004). Antitumor and antimetastatic effect of warfarin and heparins. *Biomedicine and Pharmacotherapy*, *58*, 213–219.
Chandrasekar, D., Sistla, R., Ahmad, F. J., Khar, R. K. & Diwan, P. V. (2007). Folate coupled poly(ethyleneglycol) conjugates of anionic poly(amidoamine) dendrimer for inflammatory tissue specific drug delivery. *Journal of Biomedical Materials Research A*, *82*, 92–103.
de Wolf, F. A. & Brett, G. M. (2000). Ligand-binding proteins, their potential for application in systems for controlled delivery and uptake of ligands. *Pharmacological Reviews*, *52*, 207–236.
Du, Z., Pan, S., Yu, Q., Li, Y., Wen, Y., Zhang, W., et al. (2010). Paclitaxel-loaded micelles composed of folate-poly(ethylene glycol) and poly(γ-benzyl-L-glutamate) diblock copolymer. *Colloids and Surfaces A-Physicochemical and Engineering Aspects*, *353*, 140–148.
Goldspiel, B. R. (1997). Clinical overview of the taxanes. *Pharmacotherapy*, *17*, 110S–125S.
Huh, K. M., Min, H. S., Lee, S. C., Lee, H. J., Kim, S. & Park, K. (2008). A new hydrotropic block copolymer micelle system for aqueous solubilization of paclitaxel. *Journal of Controlled Release*, *126*, 122–129.
Kim, S. Y., Shin, I. G., Lee, Y. M., Cho, C. S. & Sung, Y. K. (1998). Methoxy poly(ethylene glycol) and epsilon-caprolactone amphiphilic block copolymeric micelle containing indomethacin. II. Micelle formation and drug release behaviours. *Journal of Controlled Release*, *51*, 13–22.
Kukowska-Latallo, J. F., Candido, K. A., Cao, Z. Y., Nigavekar, S. S., Majoros, I. J., Thomas, T. P., et al. (2005). Nanoparticle targeting of anticancer drug improves therapeutic response in animal model of human epithelial cancer. *Cancer Research*, *65*, 5317–5324.
Leamon, C. P., Cooper, S. R. & Hardee, G. E. (2003). Folate-liposome-mediated antisense oligodeoxynuleotide targeting to cancer cells: Evaluation in vitro and in vivo. *Bioconjugate Chemistry*, *14*, 738–747.
Li, L., Huh, K. M., Lee, Y. K. & Kim, S. Y. (2009). Design of multifunctional heparin-based nanoparticle system for anticancer drug delivery. *Macromolecular Research*, *18*, 153–161.
Liebmann, J., Cook, J. A. & Mitchell, J. B. (1993). Cremophor EL, solvent for paclitaxel, and toxicity. *Lancet*, *342*, 1428.
Lin, J. J., Chen, J. S., Huang, S. J., Ko, J. H., Wang, Y. M., Chen, T. L., et al. (2009). Folic acid-Pluronic F127 magnetic nanoparticle clusters for combined targeting, diagnosis, and therapy applications. *Biomaterials*, *30*, 5114–5124.
Linhardt, R. J. (1991). Heparin: An important drug enters its seventh decade. *Chemistry and Industry*, *2*, 45–50.
Maeda, H., Sawa, T. & Konno, T. (2001). Mechanism of tumor targeted delivery of macromolecular drugs, including the EPR effect in solid tumor and clinical overview of the prototype polymeric drug smancs. *Journal of Controlled Release*, *74*, 47–61.
Mousa, S. A. & Petersen, L. J. (2009). Anti-cancer properties of low-molecular-weight heparin: Preclinical evidence. *Thrombosis and Haemostasis*, *102*, 258–267.
Niers, T. M., Klerk, C. P., Dinisio, M., van Noorden, C. J., Büller, H. R., Reitsma, P. H., et al. (2007). Mechanisms of heparin induced anti-cancer activity in experimental cancer models. *Critical Reviews in Oncology/Hematology*, *61*, 195–207.
Pan, J. & Feng, S. S. (2008). Targeted delivery of paclitaxel using folate-decorated poly(lactide)-vitamin E TPGS nanoparticles. *Biomaterials*, *29*, 2663–2672.
Panchagnula, R. (1998). Review: Pharmaceutical aspects of paclitaxel. *International Journal of Pharmaceutics*, *172*, 1–15.
Saul, J. M., Annapragada, A., Natarajan, J. V. & bellamkonda, R. V. (2003). Controlled targeting of liposomal doxorubicin via the folate receptor in vitro. *Journal of Controlled Release*, *92*, 49–67.
Shuai, X., Merdan, T., Schaper, A. K., Xi, F. & Kissel, T. (2004). Core-cross-linked polymeric micelles as paclitaxel carriers. *Bioconjugate Chemistry*, *15*, 441–448.
Smorenburg, S. M. & van Noorden, C. J. (2001). The complex effects of heparins on cancer progression and metastasis in experimental studies. *Pharmacological Reviews*, *53*, 93–105.

Toffoli, G., Cernigoi, C., Russo, A., Gallo, A., Bagnoli, M. & Boiocchi, M. (1997). Over-expression of folate binding protein in ovarian cancers. *International Journal of Cancer*, *74*, 193–198.

Wang, Y., Tang, L., Li, C., Xiong, M. & Wang, J. (2008). Self-assembled micelles of biodegradable triblock copolymers based on poly(ethyl ethylene phosphate) and poly(ε-caprolactone) as drug carriers. *Biomacrmolecules*, *9*, 388–395.

Zhao, P., Wang, H., Yu, M., Cao, S., Zhang, F., Chang, J., et al. (2010). Paclitaxel-loaded, folic-acid-targeted and TAT-peptide-conjugated polymeric liposomes: In vitro and in vivo evaluation. *Pharmaceutical Research*, *27*, 1914–1926.